Scripta Materialia 214 (2022) 114683

Contents lists available at ScienceDirect

Scripta Materialia

journal homepage: www.journals.elsevier.com/scripta-materialia

# On/off directional solidification of near peritectic TRIS-NPG with a planar but tilted solid/liquid interface under microgravity conditions

Andreas Ludwig [a,*], Johann Mogeritsch [a], Markus Rettenmayr [b]

[a] Lehrstuhl für Simulation und Modellierung Metallurgischer Prozesse, Department Metallurgie, Montanuniversitaet Leoben, A-8700 Leoben, Austria
[b] Lehrstuhl für Metallische Werkstoffe, Otto-Schott-Institut für Materialforschung, Friedrich-Schiller-Universität Jena, D-07743 Jena, Germany

ARTICLE INFO

*Keywords:*
Bridgman technique
Directional solidification
Optical microscopy
Interface segregation
Peritectic alloy

ABSTRACT

Understanding phenomena that occur during gradient annealing and initial transient of Bridgman-type directional solidification processes is essential for producing high-performance materials with specific properties. An experiment with alternating long time gradient annealing and directional solidification periods was performed on the International Space Station, using a near-peritectic transparent TRIS-NPG alloy. It transpired that accumulation of solute ahead of the solid/liquid interface continued to progress and that steady-state growth conditions were never achieved. The results demonstrate that (i) liquid being squeezed out from the mush during the long time gradient annealing period disables the formation of a flat interface; (ii) a thermal bias caused a slightly tilted planar solidification front; and (iii) growth of the metastable pro-peritectic α-phase led to the formation of a supersaturated solid that solidified with an intriguing low growth rate.

A Bridgman-type directional solidification experiment is generally initiated by directional melting in a temperature gradient, followed by a thermal stabilization phase that generates well-defined initial conditions in the form of a planar solid/liquid interface. After applying the temperature gradient, the sample gets partly liquid, partly both liquid and solid (mushy region), and partly solid. Initially, the mushy region is bounded by the liquidus temperature on the hot side and the solidus temperature on the cold side. However, the concentration profile in the mushy region leads to solute diffusion accompanied by local re-solidification [1] so that the concentration at the mush/liquid interface gradually increases and the concentration at the mush/solid interface gradually decreases [2,3,4,5,6]. This process continues until a flat interface that is located somewhere between liquidus and solidus establishes. Combeau et al. [3] suggested an analytical approximation to describe this phenomenon and Fischer et al. [4] experimentally verified the corresponding model for an Al-4wt.% Cu alloy.

Xu et al. [5] placed a dilute, organic Succinonitril-Camphor alloy stationary in a thermal gradient stage. They found that, after a thermal equilibrium was reached, the solid continued to melt until a certain temperature below liquidus was reached. Then, resolidification occurred until the interface velocity slowly approached zero and the interface temperature asymptotically reached a temperature level still somewhat lower than liquidus. The motion to a higher temperature level was attributed to the motion of liquid droplets of high solute concentration due to TGZM (temperature gradient zone melting) [2]. Those droplets got finally incorporated into the liquid at the interface and hence caused the liquid interface composition to increase. Resolidification was attriuted to the establishing of solute profiles in liquid and solid. This back and forth of the mush/liquid interface was confirmed by Phillion et al. [6] by comparing results from a volume-average- and a phase-field-model to experimental ESRF[1] data. Besides droplet motion by TGZM, both their phase-field predictions and ESRF observations detected the formation of liquid channels that closed only at the end of the solutal balancing stage. In the present work, to achieve this stage for our TRIS-NPG alloy, a holding time of 8 hours was selected. However, as will be demonstrated in this contribution, we did not achieve a planar solid/liquid interface during this period.

When pulling starts with a rate that ensures a morphologically stable solid/liquid interface, the solidification dynamics undergo a so-called initial transient before a steady-state is established. During this initial transient, a solute boundary layer develops due to the imbalance between the rate of rejection of solute from the interface and the rate of diffusive transport away from the interface. The corresponding solute pileup initially increases during the transient regime, and then remains

* Corresponding author at: Montanuniversitaet Leoben, Franz-Josef Strasse 18, 8700 Leoben, Austria
*E-mail address:* ludwig@unileoben.ac.at (A. Ludwig).
[1] ESRF: European Synchrotron Radiation Facility.

https://doi.org/10.1016/j.scriptamat.2022.114683
Received 2 December 2021; Received in revised form 9 February 2022; Accepted 15 March 2022
Available online 22 March 2022

constant when the planar interface reaches steady growth conditions. A quantitative understanding of the initial transient is important for many solidification and crystal growth processes as products with uniform composition can only be obtained when the initial transient is terminated. Fabietti et al. [7] conducted experiments showing that the classical models for describing the initial transient [8,9], employed the unrealistic assumption that the interface response to the change of the external velocity was instantaneous. However, in reality, the interface velocity increases gradually. This fact was accounted for in later models of the initial transient [10,11,12], but they still retained the assumption of no diffusion in the solid, no thermal lag in the system, and a uniform composition in the liquid when solidification commenced. Fabietti et al. [7] demonstrated that accounting for an initial boundary layer was necessary to find a correlation between model predictions and experimental findings. The present contribution reveals that conditions might exist where the transient build-up of a boundary layer may take longer than expected.

Between March 17, and April 24, 2021, several cartridges filled with TRIS-NPG[2] alloys of near peritectic compositions were processed by using the 'Transparent Alloy' (TA) insert to the Microgravity Science Glovebox (MSG) of the European Space Agency (ESA) onboard the International Space Station (ISS). Here, we report about a single directional solidification experiment using a TRIS-NPG alloy with $C_0 = 53$ mol% NPG and a pulling velocity that ensured a morphologically stable solid/liquid interface (TAC4S3 processed between April 20, 2021, 18:32 GMT and 22 April 22, 2022, 06:37 GMT). The experiment was performed by keeping the material immobilised in a temperature gradient of $G = 3\pm1$ K/mm for 8 hours (gradient annealing), and then pulling the sample for 8 hours with $V = 0.08$ μm/s $= 0.288$ mm/h. After that, the same was repeated one more time. Finally, the sample was kept at rest for further 4 hours. The purpose of this procedure was to clarify some observations that were made during peritectic coupled growth (PCG) under microgravity (μg-)conditions, which will be reported elsewhere. The microgravity level during the processing time of TAC4S3 was measured with the 'es09'-sensor at the MSG's 'Ceiling Right Side'. The mean μgRMS[3] was around 2.2 μg between 08:00 and 22:00 GMT and less than 0.5 μg during 'night time' of the astronauts. The median frequency measured by the sensor was roughly constant at around 0.182 Hz.

The TA apparatus was designed by ESA and was built by QinetiQ Space to serve four different ESA MAP-teams (i.e. CETSOL, METCOMP, SEBA, and SETA) for their solidification investigations using transparent metal-like solidifying alloys [13]. The technical features related to safety and automation constraints are not mentioned in this report. A cartridge with a rectangular cross-section ($10 \times 1$ mm$^2$; length: 100 mm) and optically flat fused-silica walls (Hellma), with 2.5 mm in thickness, was filled (performed by QinetiQ Space) with the molten alloy prepared with purified compounds under a protective atmosphere, and then sealed. The temperature gradient was established between two metallic blocks, separated by a 7 mm gap, each of them made of two pieces with independent thermal regulators, and good contact with the cartridge walls.

Images of the solid/liquid interface were taken perpendicularly to the front window, every half minute, and with three different focus points: directly at the front window (i.e. $ff = 0$ mm), at the middle of the sample (i.e. $ff = 0.5$ mm), and near the rear window (i.e. $ff = 0.8$mm). However, three images were broadcasted to earth only every hour. The present contribution is based on these image sequences. TA operations were essentially automated with telescience (e.g., control over parameters and sampled image series) from the operation centre (E-USOC, Madrid, Spain) permitting near real-time feedback. Although the inner length of the cartridge was 100 mm, only 66 mm was used for the solidification experiments to ensure a sufficient overlap with the hot and cold clamps. This length was conceptually separated into 6 segments, each one 11mm in length. The solidification experiments were done only with 'fresh' segments that had never been melted before.

Fig. 1 shows an example of the initial microstructure that occurred after the gradient had been activated. The solid that was in direct contact with the liquid consisted of many small grains. In addition, many bubbles could be seen, which formed a kind of a substructure in the solid. Occasionally, larger bubbles were also observed in the solid/mush close to the melt. Some of the smaller bubbles, as well as tracers in the liquid have been followed during the course of the present experiment. The origin of the tracers is not clear. They might be contaminants that were already present in the purchased components. However, they were quite small and thus difficult to observe. The bubbles and tracers that were followed were not sticking to the glass walls as they moved at different speeds compared to the cartridge, especially during the first 8 hours where the sample was at rest.

Fig. 2 shows the displacements of (i) bubbles that were located in the solid; (ii) tracers that were located in the liquid; and (iii) the solid/liquid interface observed with focus on the front window ($ff = 0$ mm) and with focus near the rear window ($ff = 0.8$ mm). As different bubbles moved identically, their movement can be seen as representing the motion of the solid. Given that under μg-conditions buoyancy does not play a role, the movement of the tracers can be seen as representing the motion of the liquid. Note that different tracers move identically except during the first 8 hours of the sample resting. It is also worth mentioning that during pulling the liquid (tracers) moved by around 3.5% faster than the solid (bubbles) in order to compensate for the solidification shrinkage.

Firstly, processes that occur during the first 8 hours of gradient annealing will be discussed. To realise the desired temperature gradient, a part of the sample was heated to 106°C (cold side) and separated from the hot clamps by a 7 mm gap (observation window). The remaining part was heated to 166°C (hot side). The side of the sample exposed to the higher temperature melted rapidly. In the cold part of the sample, however, several processes occurred while and after it heated up. Naturally, the material expands on heating until it reaches thermal equilibrium. This may happen within the first hour, as indicated by the simultaneous motion of bubbles, tracers, and the solid/liquid interface towards larger positions (Fig. 2). Surprisingly, after one hour, the displacement of the bubbles and tracers showed an opposite behaviour as they begin to shift towards lower positions (higher temperatures).

In order to understand this finding, it is paramount to refer back to the TRIS-NPG phase diagram. At low temperatures, the microstructure of a TRIS-NPG alloy with $C_0 = 53$ mol% NPG is composed in equal parts of the two faceted phases O and M. The O-phase consists of 100% TRIS, and the M-phase consists of 100% NPG. On heating, the O-phase transforms into the plastic α-phase (TRIS-rich phase that has a certain solubility for NPG) and the M-phase morphs into the plastic β-phase (NPG-rich phase that has a certain solubility for TRIS).

The phase diagram suggests that the transition from the M-phase into the β-phase commences at 310K (=37°C). However, according to Barrio et al [14]., this transformation takes several hours. The authors reported that in the case of rapid heating, as considered here, both the O- and M-phases remained until a temperature of 392.5K (=119.5°C) was reached. Then, for a $C_0 = 53$ mol% NPG alloy, they transformed into 23 mol% α- and 77 mol% β-phases. In the present work, as the temperature of the cold clamp lies between the two relevant temperatures (i.e. 37°C and 119.5°C), the transition of the facetted O- and M-phases is still ongoing during the first 8 hours of gradient annealing. The important fact is that both facetted phases reveal an approximately 10% higher density compared to the plastic α- and β-phases. Therefore, the transition from the facetted phases to the plastic phases results in expansion, and so the solid that can be seen in the observation window is pushed towards the liquid, where there is less resistance against the expansion.

The liquid also followed the motion of the solid. However, occasionally we observed tracers that were moving faster than the solid. Obviously, liquid channels that exist between the elongated grains [6] are sources of local flow which transport the liquid out of the mushy

[2] TRIS: Tris(hydroxymethyl)aminomethane; NPG: Neopentyl glycol.
[3] RMS: root-mean-square acceleration.

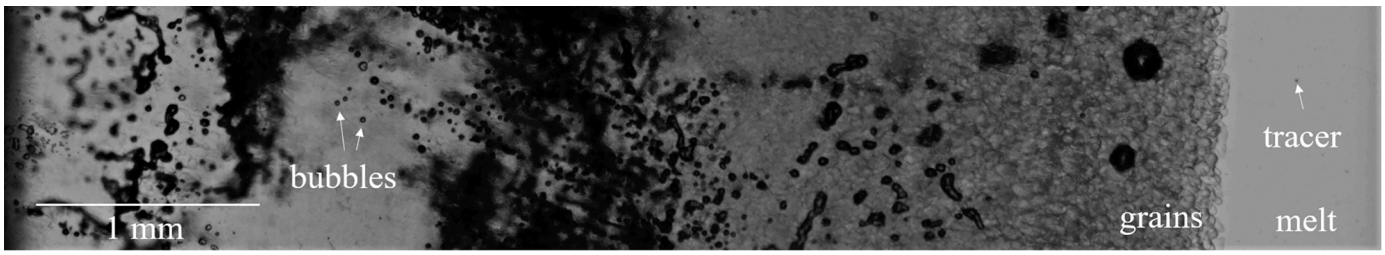


**Fig. 1.** Microstructure obtained just after the gradient had been activated (hot: right, cold: left). The melting solid consisted of many small grains that immediately started to coarsen and elongate with time. The substructure of bubbles in the solid gradually dissolved at higher temperatures. Sometimes tracers of unknown origin were visible in the melt.

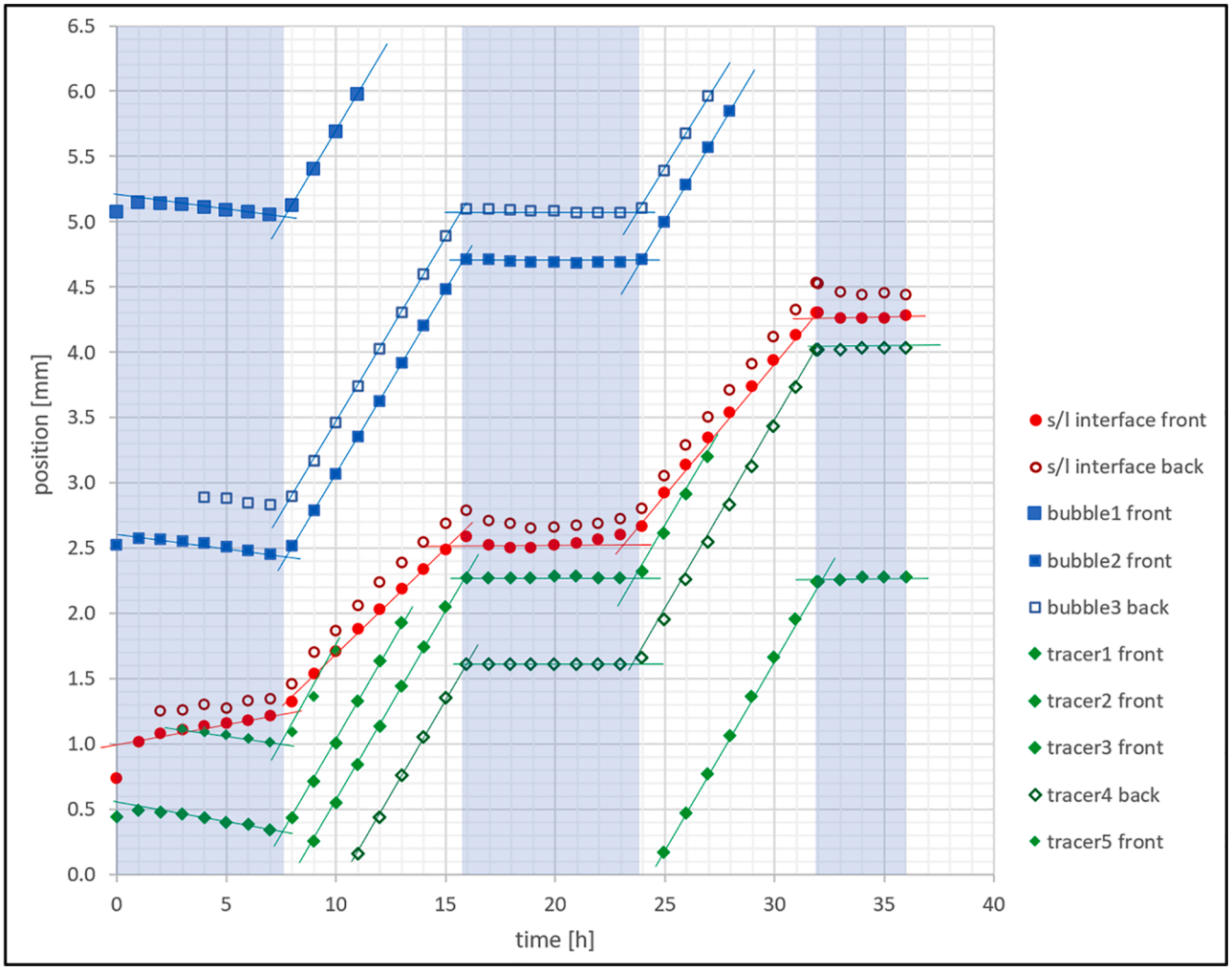


**Fig. 2.** Position of bubbles, tracers and solid/liquid interface as function of time. Blue areas indicate the cartridge at rest, whereas white areas indicate the cartridge being subjected to constant pulling. Obviously, the interface is tilted with the foremost part at the front window and the backmost part at the rear window.

zone. As the intergranular melt is enriched in solute, the liquid that is squeezed out increases the solute concentration ahead of the grain/liquid interface. A higher alloy concentration results in a lower liquidus temperature and thus leads to a displacement of the grain/liquid interface to lower temperatures, which is what happened during the experiment (see Fig. 2). During the 8 hours of gradient annealing, the grain/liquid interface is displaced by around 0.6 mm towards larger positions although bubbles and tracers move towards lower positions.

Actually, we have reported about liquid that is leaving the mushy zone via micro-channels previously [15]. At that time, we though that those micro-plumes, as we called them, were created by solutal buoyancy of highly segregated melt. The present experiment now excludes buoyancy and suggests a phase transition-induced expansion as origin for motion during the thermal gradient stage.

Fig. 3 shows the evolution of the interface at the end of the gradient annealing process. With an assumed temperature gradient of $G = 3\pm1$ K/mm and a liquidus slope of -0.48K/mol% for the α-phase, and of -0.31K/mol% for the β-phase, the increase in solute is estimated to be around 3.7 mol% for α and 5.8 mol% for β. In both cases, the solute composition at the grain/liquid interface has thus increased from 53 mol % NPG to around 57 mol% NPG or even 59 mol% NPG. This is outside the peritectic plateau, which ends at 54 mol% NPG. So, at the end of the

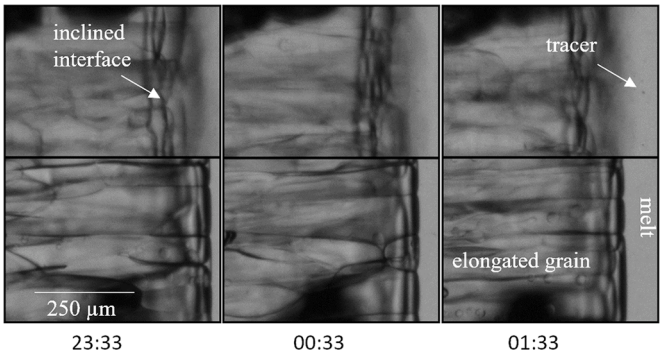


**Fig. 3.** Evolution of the mush/liquid interface after 5 hours (left), 6 hours (middle) and 7 hours (right) of keeping the sample at rest in a given temperature gradient. Upper part with focus on the middle plane ($ff = 0.5$), and lower part with focus on front plane ($ff = 0$) for the same position. The interspatial liquid channels cannot be clearly recognised. However, they have manifest themselves by tracers that left the mush as can be seen at the top right.

first 8 hours of gradient annealing, the solid phase that is in equilibrium with the liquid should be the β-phase. However, α- and β-phases are optically indistinguishable and thus it cannot be decided whether the solid grains, shown in Fig. 3, consist of α-, β- or both phases.

From the fact that the solid/liquid interface at the back is always at lower temperatures compared to the interface at the front (Fig. 2), it is evident that a thermal bias was present during the experiment. Obviously, cooling of the rear clamp of the cold zone was more effective than cooling of the front clamp. Or alternatively, the rear clamp of the hot zone is heated more intensely than the front clamp. This did not happen on purpose. However, in all sixteen TRIS-NPG experiments using the TA-apparatus, we made similar observations. If the minimum value of the position difference is taken as a reference value, the tilt angle of the isotherm can be quoted as -6.9±0.5° for the present experiment, which is a similar value as the one stated in [16] for their recent usage of the TA apparatus onboard of the ISS.

During the full 36 hours of processing, the solid/liquid interface is tilted with the foremost part at the front window and the rearmost part at the back. Fig. 4. displays the difference in position and the corresponding growth velocity as function of time. Fig. 5a exhibits an example of the tilted interface. Note that the strength of the inclination oscillates with increasing values during pulling and decreasing ones during being at rest (Fig. 4a).

In order to discuss these findings, it is helpful to recall the analysis of the former microgravity solidification experiments published by Mota et al. [17]. In their experiments, they directionally solidified a Succinonitrile-Camphor alloy in a cylindrical crucible with an inner diameter of 10 mm. They nicely demonstrated that an interface recoil might have three contributions: (i) solutal recoil, (ii) instrumental recoil, and (iii) latent heat effect. The instrumental recoil is caused by an isotherm shift due to pulling. The latent heat effect is of importance when the sample material has a lower thermal conductivity compared to the container walls as e.g. in the present case ($\lambda_{glass} = 1.7$ W/m/K and $\lambda_{NPG} = 0.25$ W/m/K). Then evacuation of latent heat mainly occurs through the container walls and thus induces a thermal radial gradient from the border (colder) to the centre (hotter) of the crucible. The effects of instrumental recoil and latent heat release are both roughly proportional to the pulling rate, and they both increase the concavity of the interface. However, for growth velocities smaller than $V = 1$ µm/s they might be negligible, at least for the experimental conditions presented in Ref. [17].

In the present experiments, the TA cartridge is flat rather than cylindrical. Although the 1 mm distance between the glass walls is quite thick compared to other flat solidification samples, heat extraction might be more effective than in the DECLIC device used by Mota et al. [17]. In addition, the fact that the interface is and remains tilted demonstrates that cooling from one side is more effective and that this thermal bias is more important than the latent heat effect. A possible instrumental recoil for the present investigation will be discussed later.

Another topic that must be discussed when comparing the current work with the experiments of Mota et al. [17] is the possibility of residual convection. The authors observed that for a pulling rate as small as $V = 0.5$ µm/s, the interface recoil did not stop even after over 30 hours of processing. They attributed this finding to the occurrence of residual convection obtained in a reduced gravity environment, like the $10^{-4}$g of their experiments. As stated above, in the present study, the g-level was in the microgravity range and, more convincing, we have never observed any large-scale convection pattern by watching the trajectories of the tracers (only feeding flow and squeezing out of liquid from mushy zone channels were detected).

From Fig. 4a, it is obvious that the inclination of the solid/liquid interface increased with time during pulling and decreased during sample resting. This can be caused by a thermal or solutal reason. It is conceivable that, during pulling, the heat transfer between the cartridge wall and the cooler/heater clamps in the back might change differently compared to the front and thus the isotherms tilt even more. This process should be reproducible when pulling stops, as confirmed by Fig. 4a. The other origin of the increase in inclination might be caused by lateral solute diffusion along the front. For a tilted solid/liquid interface, the diffusion away from the front into the bulk melt reveals a longitudinal and a lateral component. The lateral component is, however, constrained by the container walls. This constraint leads to a segregation of solute at the rearmost part of the interface and a depletion at the foremost part. As this phenomenon continues during pulling over time, the inclination of the interface increases. However, even under such conditions, a steady-state is possible and the final inclination should become constant on a somewhat higher level compared to the thermal bias. This was proven by recent phase-field simulations [18]. Also, this effect is reproducible when pulling stops, so that the inclination might oscillate between a thermally given bias value at rest and an increased solutally induced inclination during pulling. Note that generally, thermally activated processes happen much faster than solutally activated ones. It is also worth mentioning that a thermally activated increase in the interface inclination will also have a solutal response.

Another interesting finding is the fact that after pulling stops, the tilted interface continues to grow, as shown in Fig. 4b. Again, this might have a thermal or a solutal reason. It is known that a thermal shift describing the instrumental recoil might be time-dependent [17]. However, a time delay of several hours as indicated by Fig. 4b seems unrealistic. It seems more natural to consider an rearrangement of solute ahead of the front. Fig. 4a shows that after 8 hours of sample in rest, the inclination reduces nearly by half. However, the interpretation of this finding is again complex as 3 to 4 hours after stopping, grain boundaries become visible at the solid/liquid interface (see Fig. 5b). As solute diffuses from these grain boundaries towards the bulk melt, the average concentration at the solid/liquid interface increases again and thus the interface moves slightly to regions with lower temperatures and thus larger positions (Fig. 2). This can be seen from Fig. 4b as the growth velocity changes sign from positive to negative. In other words, the diffusive reduction of both solute pileup and lateral segregation is superimposed by a new source of solute, namely from 'wet' grain boundaries. The fact that these boundaries became visible only with decreasing growth velocity indicates that solidification close to the grain boundaries did indeed create a supersaturated solid that tends to equilibrium (melting) under suitable conditions. This concept was already discussed in [1]. Surprisingly, after around 7 hours at rest also droplets in the solid occurred (Fig. 5b). This fact also indicates supersaturation in the solid even away from the grain boundaries. The 'wet' grain boundaries as well as the droplets immediately disappear when pulling recommences.

The existence of supersaturated solid that has formed during such slow growth rates is quite surprising. As stated above, for the solute

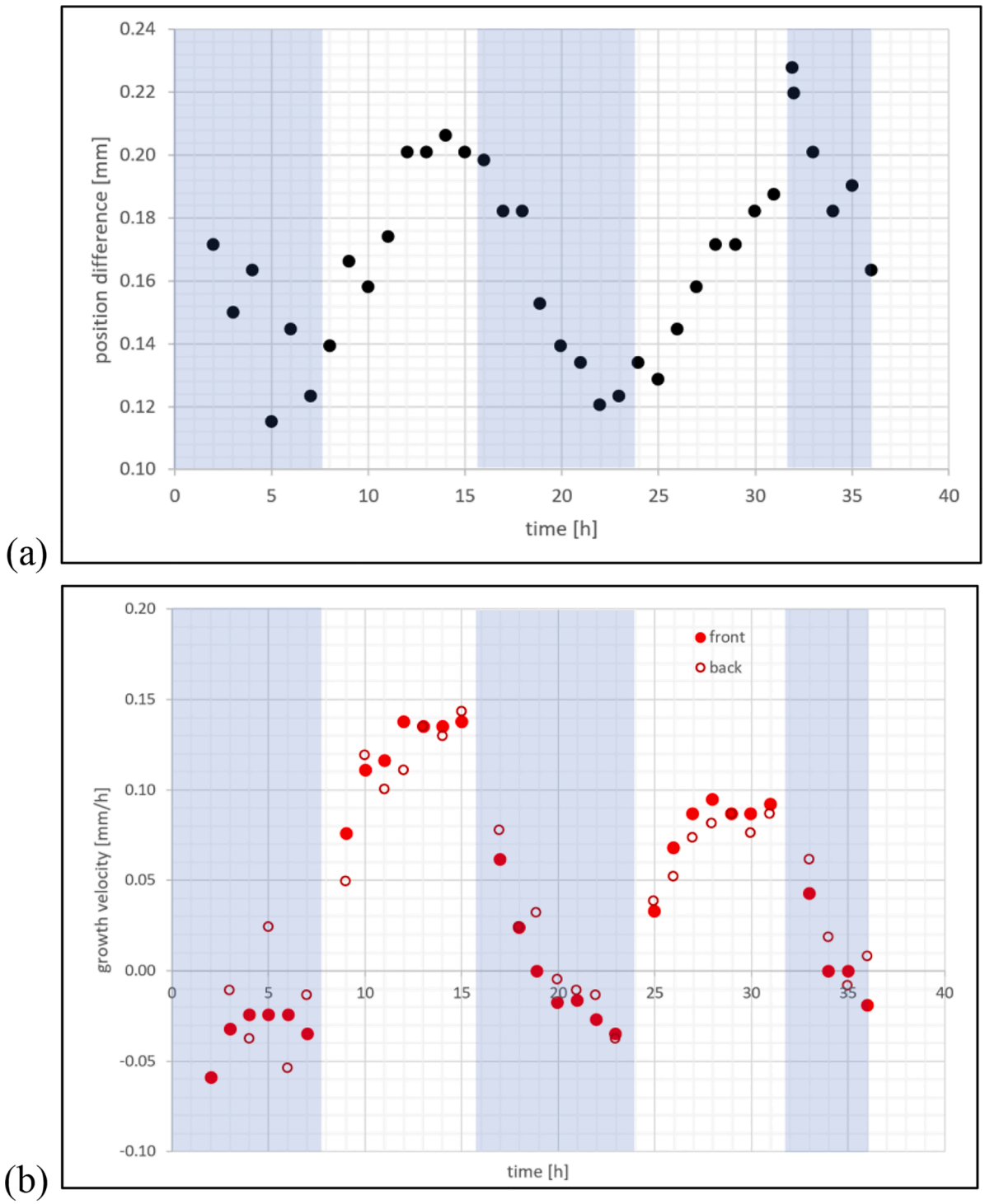


**Fig. 4.** (a) Oscillatory inclination of the solid/liquid interface indicated by the difference in position of the foremost and the rearmost front as function of time. During growth, the inclination increases, whereas during sample resting it decreases. (b) Growth velocity of the solid/liquid interface as function of time for both the front and the back part of the interface.

concentrations present at the interface only the β-phase can be in equilibrium with the liquid. However, growth of β under the present conditions would not produce a supersaturated solid. We are thus convinced that the α-phase is the solidifying phase shown in Fig. 5. According to the phase diagram, for $C > 54$ mol% NPG the α-phase is metastable and thus supersaturated. Nucleation hindrances for the β-phase in the TRIS-NPG system are well known. As the metastable solidus of the α-phase is a priori not known, it is conceivable that the long lasting interface recoil presented in Fig. 2 belongs to the initial transient of the metastable α-phase.

Fig. 4b shows that after initial pulling, the tilted solid/liquid interface starts to move at an increasing growth velocity. However, even after 8 hours of pulling, the growth velocity is still around half of the pulling speed of $V = 0.08$ μm/s $= 0.288$ mm/h for the first pulling period and around one third of the pulling speed for the second pulling period. Obviously, the initial transient of the metastable α-phase is still ongoing.

In conclusion, it must be stated that to achieve steady-state directional solidification with a planar solid/liquid interface requires much

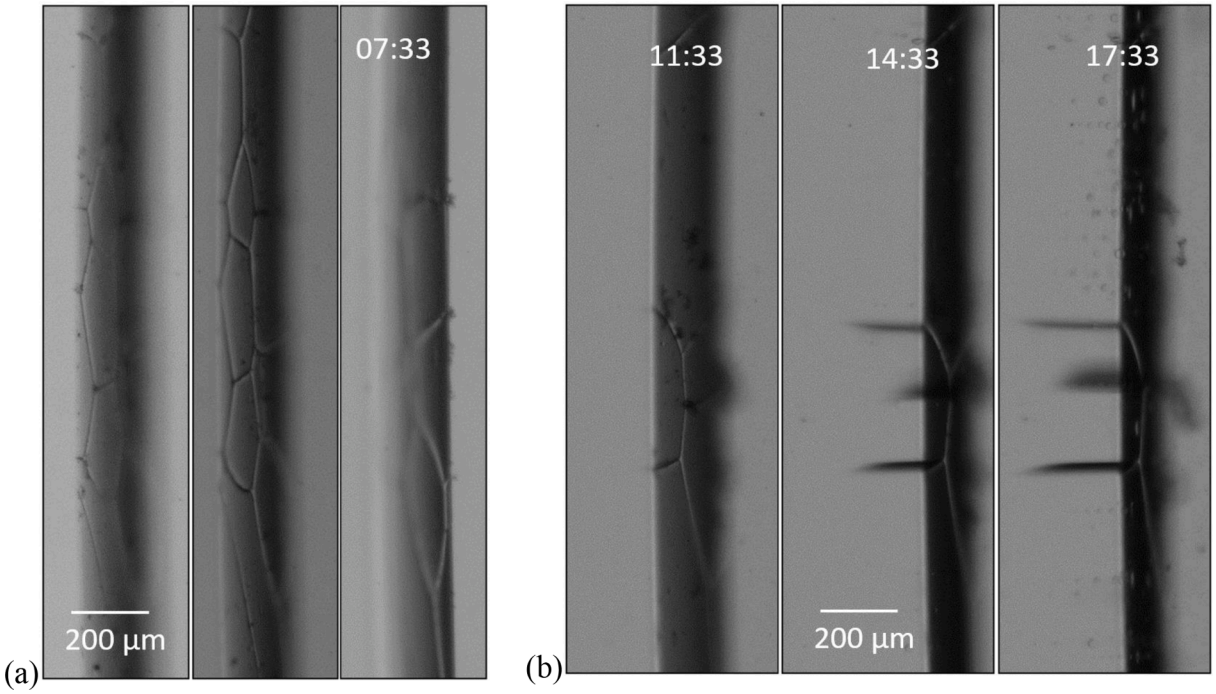


**Fig. 5.** (a) Tilted solid/liquid interface taken with, from left to right, front focus, middle focus, and back focus. The images, taken after 13 hours of processing (April 21, 2021, 07:33 GMT), show a planar interface with several grain boundaries. Also, the accumulation of tracers at the grain boundaries are visible. (b) After terminating pulling at 10:20 GMT, grain boundaries melted and became visible. The segregated melt in the boundaries gradually diffuses towards the interface, changing the concentration ahead of the solid/liquid interface. Note also the formation of droplets especially at 17:33 GMT. Images were taken with a middle focus ($ff = 0.5$).

more insights than it might seem. Establishing a suitable initial situation entails a complete understanding of phenomena that arise during gradient annealing. Besides simple diffusion in the intergranular liquid of the mushy region, more complex phenomena like TGZM [2,19–22], Liquid Film Migration (LFM) [23,24], coarsening [25] and thermomigration [26] must be considered [1]. The present contribution adds a further phenomenon to this list, namely sluggish phase transformation in the 'cold' part and associated density changes.

The second, and maybe more important aspect, is that strong evidence for the growth of the metastable α-phase has been found. Obviously, nucleation hindrance inhibited the formation of the stable β-phase and so the α-phase was forced to grow with higher solute concentration as thermodynamically advised and therefore supersaturated. With an a priori unknown metastable α-solidus line, it is conceivable that the observed long lasting interface recoil belongs to the initial transient of the planar growing supersaturated α-phase.

## Declaration of Competing Interest

The authors declare that they have no known competing financial interests or personal relationships that could have appeared to influence the work reported in this paper.

## Acknowledgments

We are thankful to the European Space Agency (ESA), and QinetiQ Space (Antwerp, Belgium) for the development of the TRANSPARENT ALLOYS instrument and E-USOC at the Polytechnical University Madrid for support in performing the experiments on the International Space Station (ISS). We also acknowledge the reviewers for their helpful criticism and their elucidative questions. This research was realized thanks to the support from ESA in the frame of the project METCOMP and from the Austrian Research Promotion Agency (FFG) under grant number 865969.

## References

[1] A. Löffler, K. Reuther, H. Engelhardt, D. Liu, M. Rettenmayr, Acta Mater 91 (2015) 34–40.
[2] H. Nguyen-Thi, B. Drevet, J.M. Debierre, D. Camel, Y. Dabo, B. Billia, J. Cryst. Growth 253 (2003) 539–548.
[3] H. Combeau, B. Appolaire, J.-M. Seiler, Nucl. Eng. Des. 240 (2010) 1975–1985.
[4] S. Fischer, M. Zalodnik, J.-M. Seiler, M. Rettenmayr, H. Combeau, J. Alloy. Compd. 540 (2012) 85–88.
[5] M. Xu, L.M. Fabietti, Y. Song, D. Tourret, A. Karma, R. Trivedi, Scr. Mater. 88 (2014) 29–32.
[6] A.B. Phillion, M. Založnik, I. Spindler, N. Pinter, C.A. Aledo, G. Salloum-Abou-Jaoude, H. Nguyen Thi, G. Reinhart, G. Boussinot, M. Apel, H. Combeau, Acta Mater 141 (2017) 206–216.
[7] L.M. Fabietti, P. Mazumder, R. Trivedi, Scr. Mater. 97 (2015) 29–32.
[8] W.A. Tiller, K.A. Jackson, J.W. Rutter, B. Chalmers, Acta Met 1 (1953) 428–437.
[9] V.G. Smith, W.A. Tiller, J.W. Rutter, Can. J. Phys. 33 (1955) 723–745.
[10] J.A. Warren, J.S. Langer, Phys. Rev. E 47 (1993) 2702–2712.
[11] B. Caroli, C. Caroli, L. Ramirez-Piscina, J. Cryst. Growth 132 (1993) 377–388.
[12] S.R. Coriell, R.F. Boisvert, G.B. McFadden, L.N. Brush, J.J. Favier, J. Cryst. Growth 140 (1994) 139–147.
[13] A. Ludwig, J. Mogeritsch, M. Kolbe, G. Zimmermann, L. Sturz, N. Bergeon, B. Billia, G. Faivre, S. Akamatsu, S. Bottin-Rousseau, D. Voss, JOM 64 (2012) 1097–1101.
[14] M. Barrio, D.O. Lopez, J.L. Tamarit, P. Negrier, Y. Haget, J. Mater. Chem. 5 (1995) 431–439.
[15] J.P. Mogeritsch, T. Peifer, A. Ludwig, IOP Conf. Ser. Mater. Sci. Eng. 529 (2019), 012025.
[16] S. Bottin-Rousseau, V.T. Witusiewicz, U. Hecht, J. Fernandez, A. Laveron-Simavilla, S. Akamatsu, Scr. Mater. 207 (2022), 114314.
[17] F.L. Mota, N. Bergeon, D. Tourret, A. Karma, R. Trivedi, B. Billia, Acta Mater 85 (2015) 362–377.
[18] T. Pusztai, Pers. Commun. (2022).
[19] W.G. Pfann, AIME 203 (1955) 961–964.
[20] W.A. Tiller, J. Appl. Phys. 34 (1963) 2757–2769.
[21] T.A. Lograsso, A. Hellawell, J. Cryst. Growth 66 (1984) 531–540.
[22] H.N. Thi, G. Reinhart, A. Buffet, T. Schenk, N. Mangelinck-Noel, H. Jung, N. Bergeon, B. Billia, J. Härtwig, J. Baruchel, J. Cryst. Growth 310 (2008) 2906–2914.
[23] D.N. Yoon, W.J. Huppmann, Acta Met 27 (1979) 973–977.
[24] S. Fischer, M. Rettenmayr, Int. J. Mater. Res. 102 (2011) 1226–1231.
[25] T. Kattamis, J. Coughlin, M. Flemings, AIME 239 (1967) 1504–1511.
[26] T.R. Anthony, H.E. Cline, J. Appl. Phys. 42 (1971) 3380–3387.